6

Formation of Dissipative Structures During Crystallization of Supercooled Melts

Leonid Tarabaev and Vladimir Esin*
Institute of Metal Physics, Ural Division of the Russian Academy of Sciences
Russia

1. Introduction

The process of crystallization in a system far from equilibrium has features, which manifest themselves in the morphology, crystal growth velocity, and segregation of dissolved alloy components. So under conditions of high cooling rates of melt ($R \sim 10^6$ K/s), when the deep supercoolings are reached an irregular morphology of solidification, nonequilibrium «trapping» of impurity, and coexistence of crystalline and amorphous phases observed (Miroshnichenko, 1982). For sufficiently high growth velocities, i.e. for certain critical undercooling the sharp transition to a partitionless regime of crystallization will take place (Nikonova & Temkin, 1966). It afterwards was called as kinetic phase transition (Chernov & Lewis, 1967; Chernov, 1980; Temkin, 1970). The critical supercooling can reach large values: so for Ni-B alloy of ~ 200 ÷ 300 K (Eckler at al., 1992). The dissipative structures formed in such system, essentially influence on set of main properties of prepared material.

In the continuous growth model the boundary conditions for solute partitioning at the crystal-melt interface are established (Aziz & Kaplan, 1988; Aziz, 1994; Kittl at al., 2000). These conditions are used in models to explaining the experimental data on solute trapping, in particular, in the phase-field models (Ahmad at al., 1998; Ramirez at al., 2004; Wheeler at al., 1993). The dependences of the kinetic coefficient and the diffusion rate at the interface on the temperature are not usually considered. In models of dendritic growth used for the computation of the rapid solidification kinetics (Eckler at al., 1992, 1994) the diffusion rate and the kinetic coefficient in a collision-limited form are entered as independent fitting parameters. The method of computer simulation (Tarabaev at al., 1991a) allows study the formation of a complex morphology of the solid – liquid interface and it dynamics during a crystallization of pure metals (Tarabaev at al., 1991b) and metal alloys (Tarabaev & Esin, 2000, 2001). In this work the crystallization from one centre of a binary essentially nonequilibrium system is investigated in computer model (Tarabaev & Esin, 2007) that takes into account the temperature dependence of the diffusion coefficient and the nonequilibrium partition of dissolved component of the alloy (Aziz & Kaplan, 1988).

* Corresponding Author

2. Computer model

2.1 Kinetics of crystallization

The computer model is based on a finite difference method. The two–dimensional finite-difference grid divides the system into cells. Each cell is characterized by a volume fraction of a solid phase g_S. Assuming the normal mechanism of crystal growth the velocity of an interface motion V in a two-phase cell ($0 < g_S < 1$) can be written as follows:

$$V = \beta \Delta T \ , \tag{1}$$

where β - is anisotropic kinetic coefficient, ΔT - is kinetic supercooling at the interface:

$$\Delta T = T_E - T_I = T_M(1 - d_0\kappa) - mc_I - T_I \tag{2}$$

Here T_E - is equilibrium temperature, T_M - is temperature of melting of first component, d_0 - is capillary length:

$$d_0 = \gamma_{SL}/Q \ , \tag{3}$$

Here γ_{SL} - is surface tension of crystal – melt interface, Q - is heat of melting, κ - is interface curvature, m - is the slope of the equilibrium liquidus line (without sign), T_I and c_I - are the temperature and the concentration in the liquid at the interface, respectively.

The nonequilibrium effect of solute partition at interface is described by expression (Aziz & Kaplan, 1988) for partition coefficient k:

$$k(V) = \frac{c_S}{c_L} = \frac{V/V_D + k_e}{V/V_D + 1 - (1 - k_e)c_L} \ , \tag{4}$$

where c_S and c_L - are concentration in the solid and in the liquid at the interface, respectively,

$$k_e = k_0 \ / \ k_0^A \ , \tag{5}$$

Here k_0 and k_0^A - are the equilibrium partition coefficients of solute and solvent, respectively; V_D - is the rate of diffusion:

$$V_D \equiv f\nu a \exp\left(-E_a/RT\right) = D \ / \ a \ , \tag{6}$$

Here f - is geometric factor, υ - is the atomic vibration frequency, a - is interatomic spacing, E_a - is the activation barrier for diffusion through the interface, D - is coefficient of diffusion at the interface. The partition coefficient depends on the ratio of velocity of crystallization V to rate of diffusion V_D. Rate of diffusion is the ratio of the diffusion coefficient at interface to the interatomic spacing.

The kinetic effect includes both temperature and orientation dependences of the kinetic coefficient, whose polar diagram has the four-fold symmetry and the directions of the maxima β coincide with the principal grid directions. Then the velocity of an interface motion V can be written as (Chernov, 1980; Miroshnichenko, 1982):

$$V = \beta \Delta T = f'\nu a \exp\left(-E'_a/RT\right) Q\Delta T/RT_E T \ , \tag{7}$$

where β - is the kinetic coefficient:

$$\beta = f'\nu a \exp\left(-E'_a/RT\right) Q/RT_E T \ , \tag{8}$$

f' - is a factor of anisotropy, E'_a - is the activation barrier for atomic kinetics. The ratio of the interface velocity to the diffusion rate in (4) can be written as follows

$$\frac{V}{V_D} = \frac{f'}{f} \exp\left(-\frac{E'_a - E_a}{RT}\right) \frac{Q\Delta T}{RT_E T}, \tag{9}$$

In the case when the energy of activation for atomic kinetics E'_a is equal to the energy of activation for diffusion E_a at the interface from expression (9) follows that

$$\frac{V}{V_D} = \frac{f'}{f}\left(\frac{Q\Delta T}{RT_E T}\right). \tag{10}$$

The ratio V/V_D characterizes of the deviation degree from equilibrium of the interface for given temperature ($\Delta T/T$) and entropy of melting (Q/RT_E). That is in terms of the atomic kinetics it signifies the ratio of a resulting flux of atoms to an exchange (equilibrium) flux at the interface. And the ratio (f'/f) characterizes the degree of the anisotropy of crystal growth rate. In case of $V = V_D$ from the equation (10) the expression for a supercooling follows:

$$\Delta T^* = \frac{T_E}{1 + \left(f'/f\right)\left(Q/RT_E\right)}, \tag{11}$$

which can be the criterion of transition to nonequilibrium trapping of dissolved component of the alloy at interface at supercoolings larger than this value. Graphic presentation of the equations (1, 4, 6, and 7) for the system *Fe-B* is shown in Fig. 1.

2.2 Heat - and mass transfer in a system

For each volume element Ω of a system from conservation laws follow the equations for fields of c_L , c_S , and T:

$$\frac{\partial c_L}{\partial t} = \frac{(1-k)\,c_L}{g_L}\frac{\partial g_S}{\partial t} + \frac{1}{g_L \Omega}\int_S \left(g_L D_L(T)\vec{\nabla} c_L, d\vec{S}\right), \tag{12}$$

$$\frac{\partial (c_S g_S)}{\partial t} = k c_L \frac{\partial g_S}{\partial t}, \tag{13}$$

$$\frac{\partial T}{\partial t} = \alpha \nabla^2 T + \frac{Q}{C}\frac{\partial g_S}{\partial t}, \tag{14}$$

where g_S and g_L - are fractions of solid and liquid phases, α and C – is the thermal diffusivity and capacity, respectively; the diffusion coefficient in the melt depends on the temperature:

$$D_L(T) = a^2 \nu \exp(-E_D/RT) \tag{15}$$

Here, we neglect diffusion in the solid phase and the thermal diffusivity α is accepted identical in both phases. The source in equation (14) (also in (12)) is simulated by algorithm developed in (Tarabaev at al., 1991a), using the expression for the change of a volume fraction of a solid phase in two-phase cell of a system:

$$\frac{\partial g_s}{\partial t} = \frac{V(\vec{n})l(\vec{n})}{\Omega}, \tag{16}$$

where $\vec{n}$ - is the local normal to the interface segment in a two-phase cell and l ($\vec{n}$) - is the area of the interface segment. The finite-difference scheme of the problem was formulated with regard for these equations, and the corresponding computer program was modified (Tarabaev & Esin, 2007).

We now use the dimensionless quantities:

$$\tilde{c} = (c_0/k_0 - c)/\Delta c_0, \quad \tilde{V} = V/v_0, \quad \tilde{V}_D = V_D/v_0, \quad \Delta\tilde{T} = \Delta T\ C/Q.$$

Here, c_0 - is the initial concentration of solute in melt,

$$\Delta c_0 = c_0 (1 - k_0)/k_0 v_0, \tag{17}$$

$$v_0 = \beta_0 Q/C, \tag{18}$$

β_0 - is isotropic kinetic coefficient at the phase equilibrium temperature. The relation between the diffusion rate and the kinetic coefficient at the equilibrium temperature has the form:

$$V_D(T_E) = \varepsilon \beta_0 R T_E^2 / Q, \tag{19}$$

where ε - is the factor which takes into account the difference between activation barriers for atomic kinetics and for the diffusion at the interface. We assume that

$$V_D(T_E) / \nu_0 = \varepsilon \Theta / (Q / RT_E) = 0.9\ , \tag{20}$$

here $\varepsilon = 0.31$ ($\varepsilon = 1$ at $E_a' = E_a$), and

$$\Theta = (C / Q)T_E\ . \tag{21}$$

Dependence of growth velocity $\tilde{V}$ on supercooling of the melt $\Delta\tilde{T}$ is calculated in a maximum (+) for $(f'/f)_{\max} = 1.5$ and in minimum (-) for $(f'/f) = 1$ of orientation dependence of a kinetic coefficient, which also depends on the temperature.

Velocity of crystallization $\tilde{V}_0$ as function of supercooling in case of constant kinetic coefficient (without temperature dependence) is presented in Fig. 1. At the large supercoolings (dimensionless supercoolings are more approximately 0.2) the curve calculated from (7) essentially deviates from the linear growth law. Velocity $\tilde{V}$ as a function of $\Delta\tilde{T}$ has a maximum at the supercooling:

$$\Delta\tilde{T}_{V\max} = T_E C / Q \Big/ \left(1 + E_a^{'} / RT_E\right) \tag{22}$$

We will note also, that velocity of crystallization becomes equal to the diffusion rate at values of supercooling $\Delta\tilde{T}^*$ which depend on the degree of anisotropy of kinetic coefficient that is on the ratio (f'/f) in expression (11).

Values $\Delta\tilde{T}^*$ will be smaller at $\varepsilon < 1$. All these presented above effects are known separately, but in this model they are interdependent. Taking into account the diffusion as the limiting factor, the true $\tilde{V}(\Delta\tilde{T})$-curve will lie below than these dependences are calculated from (7) in the kinetic regime of crystal growth. The kind of a curve can be obtained as a result of the computer simulation. Crystal growth is controlled by a joint action of kinetic phenomena at the interface and heat transfer and second-component mass transfer in the system.

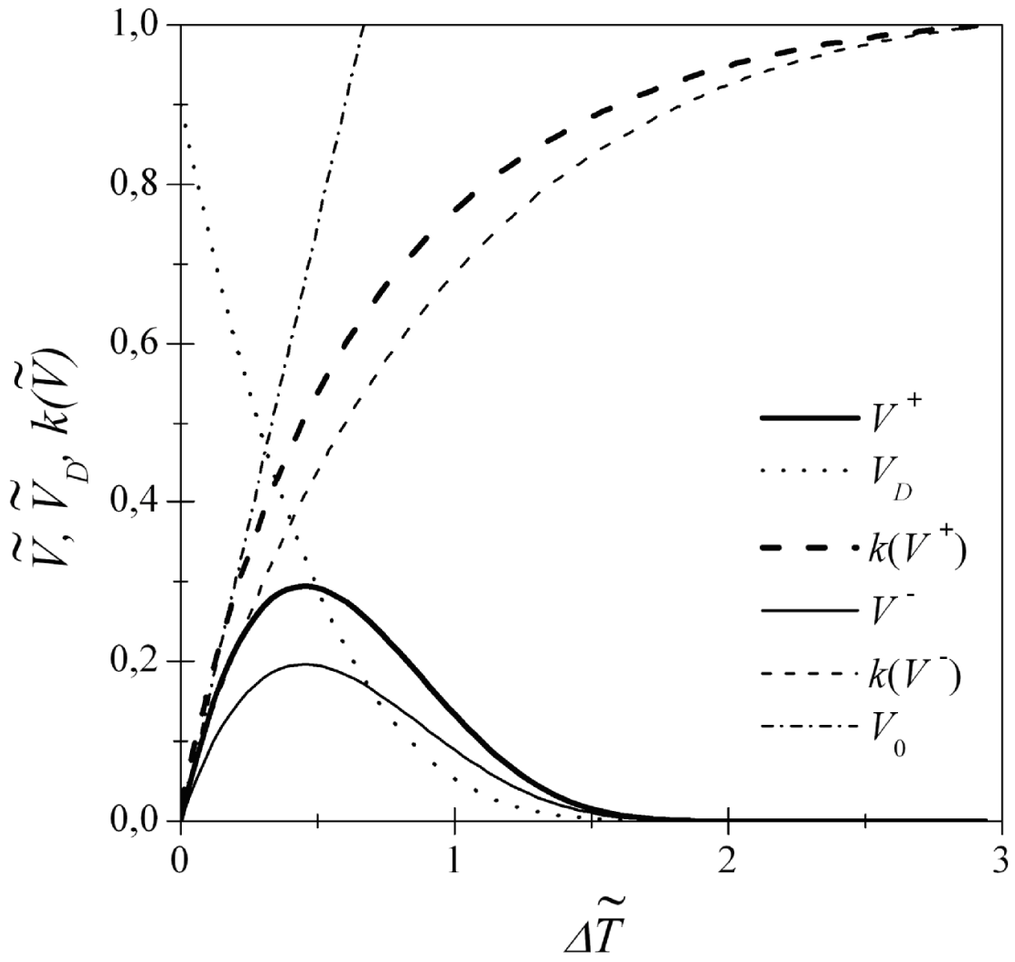

Fig. 1. Dependences of velocity of crystal growth $\tilde{V}$, diffusion rate $\tilde{V}_D$ and nonequilibrium partition coefficient k (V) on supercooling $\Delta\tilde{T}$ of the *Fe–B* melt with $\Theta = 2.96$, $E_a/RT_E = 5.55$, $Q/RT_E = 1.0$, and $k_0 = 0.015$. Curves drawn in maximum (V^+) and minimum (V^-) of the orientation dependence of kinetic coefficient (at $V^+/V^- = 1.5$).

3. Results of computer simulation

We consider the melt solidification from one centre in a two-dimensional system of different sizes (N Δh x N Δh cells). Here Δh = 0.20 (α / v_0) - is linear size of the unit cell.

The parameters of the problem approximately correspond to *Fe-B* system (Hansen & Anderko, 1957; Hain & Burig, 1983): the iron melting temperature is T_M^{Fe} = 1809 K, the liquidus temperature is T_E = 1803 K at an initial boron concentration c_0 = 0.04 wt % B ($\Theta = (C/Q)T_E$ = 2,96); E_a = 83.8 kJ/mol (E_a/RT_E = 5,55), Q = 15.38 kJ/mol ($Q/RT_E \approx 1$), Q/C = 609K, the equilibrium partition coefficient is k_0 = 0.015, and the slope of the liquidus line m = -102 K/wt %. D_L (T_E) = 5 × 10^{-9} m²/s, γ_{SL} = 0.12 J/m², α = 0.7 × 10^{-5} m²/s. The characteristic scales of the problem ware as follows: the velocity $v_0 \approx 1.2 \times 10^2$ m/s, length (α / v_0) ≈ 1 × 10^{-7} m, and time (α / v_0^2) ≈ 1 × 10^{-9} s for β_0 = 0.2 m/(s K).

3.1 Morphology of dissipative structures formed during the solidification of a supercooled melt under conditions when the crystal growth is limited by diffusion of the dissolved component

We consider the crystal growth from of a single centre in a system of 1000 × 1000 cells (Fig. 2) and in a system of 500 × 500 cells (Fig. 3-5) with the following calculation parameters: time step $\Delta\tilde{t} = (v_0^2/\alpha)\Delta t$ = 0.02 and spatial step $\Delta\tilde{h} = (v_0/\alpha)\Delta h$ = 0.20. The computer simulation is realized in the systems with a fixed supercooling $\Delta T = \Delta T_{bath}$ with adiabatic boundary. The anisotropy of the orientational dependence of the kinetic coefficient $(f') = 6$. In these calculations (in this region of the melt supercooling) does not take into account the temperature dependence of the kinetic processes in interface crystal and diffusion of solute in the melt.

Morphology of dissipative structures formed during *Fe-B* melt crystallization and concentration fields in the system in some moments of the time $\tilde{t}$ for various values of bath

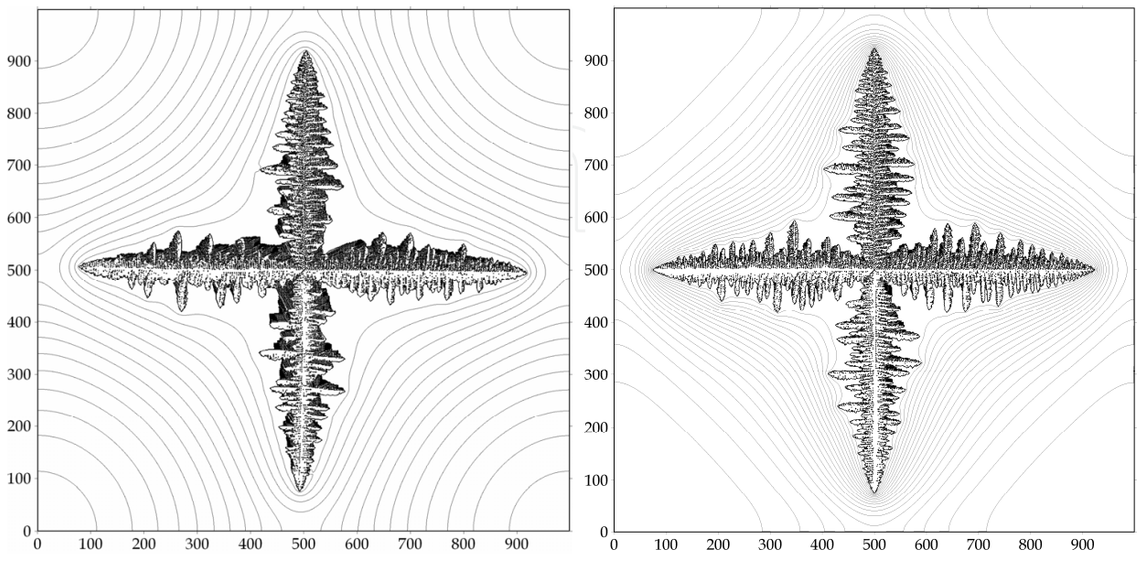

(a) (b)

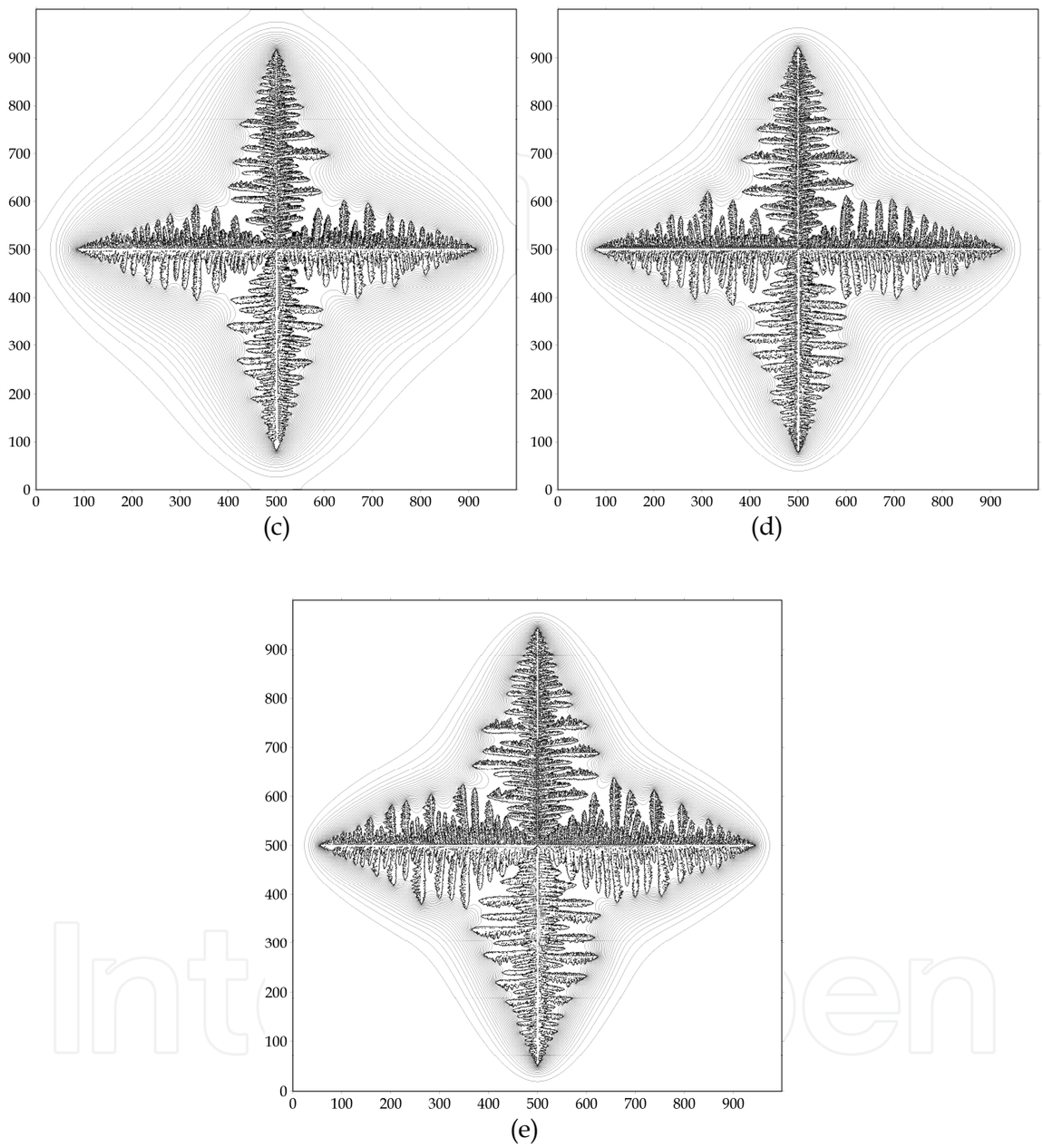

Fig. 2. Morphology of dissipative structures are formed during *Fe-B* melt crystallization and concentration fields (thin lines) in the system in some moments of the time $\tilde{t}$ for various values of bath supercooling $\Delta\tilde{T}_{bath}$: (a) $\Delta\tilde{T}_{bath}$ = 0.01, $\tilde{t}$ = 750; (b) $\Delta\tilde{T}_{bath}$ = 0.02, $\tilde{t}$ = 230; (c) $\Delta\tilde{T}_{bath}$ = 0.03, $\tilde{t}$ = 120; (d) $\Delta\tilde{T}_{bath}$ = 0.04, $\tilde{t}$ = 80; (e) $\Delta\tilde{T}_{bath}$ = 0.05, $\tilde{t}$ = 40; The isolines of the dimensionless concentration ($\tilde{c}$) were plotted with intervals: (a) $\Delta\tilde{c}$ = 0.005, (b),(c) $\Delta\tilde{c}$ = 0.010, and (d),(e) $\Delta\tilde{c}$ = 0.020, respectively.

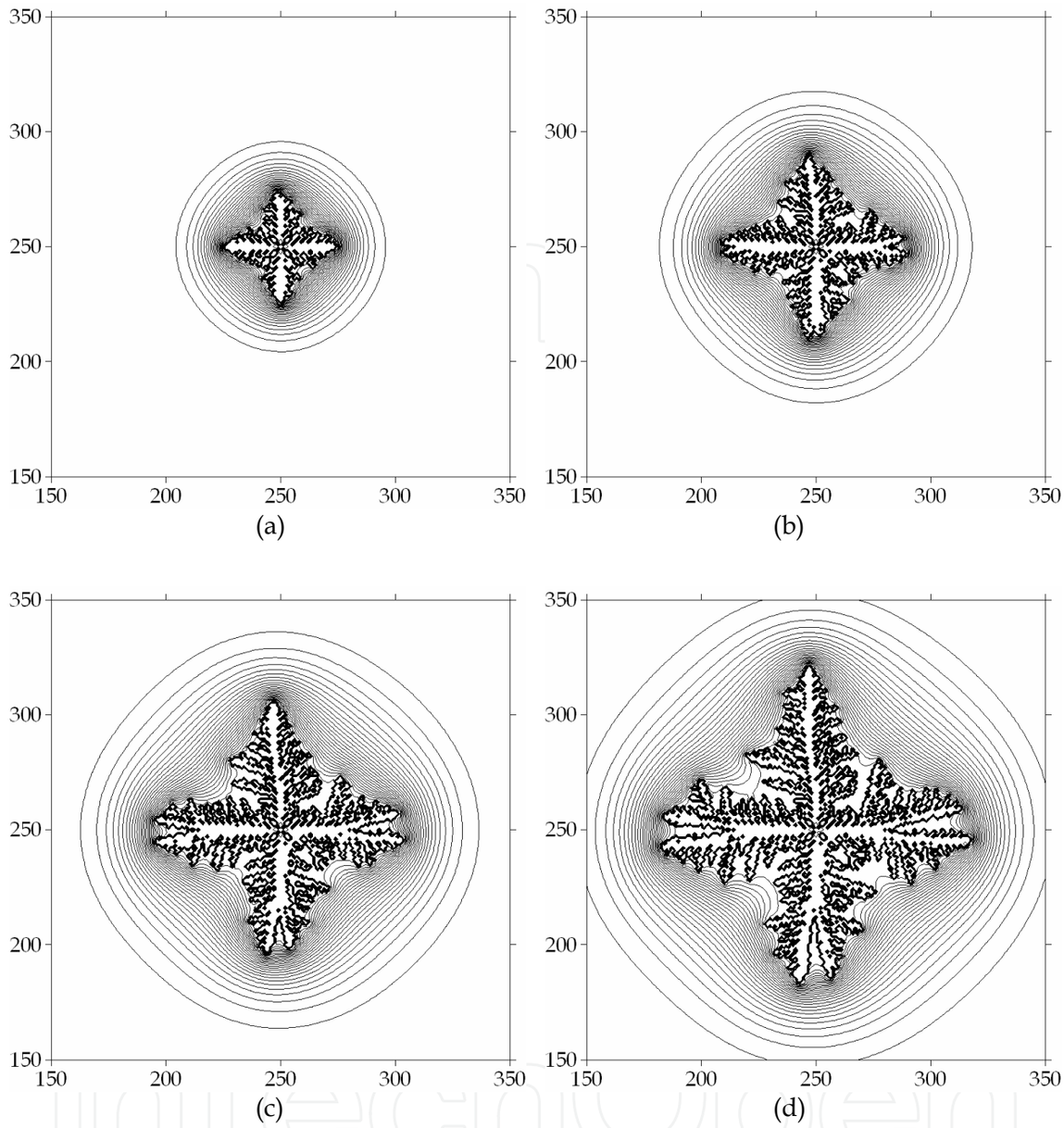

Fig. 3. Morphology of dissipative structures are formed during *Fe-B* melt crystallization and concentration fields (thin lines) in the system in some successive moments of the time $\tilde{t}$ for value of bath supercooling $\Delta\tilde{T}_{bath}$ = 0.055: (a) $\tilde{t}$ = 5, (b) $\tilde{t}$ = 10, (c) $\tilde{t}$ = 15, and (d) $\tilde{t}$ = 20. The isolines of the dimensionless concentration ($\tilde{c}$) were plotted with $\Delta\tilde{c}$ = 0.02 intervals.

supercooling $\Delta\tilde{T}_{bath}$ are shown in Fig. 2-5. Analysis of the evolution of dissipative structures change with supercooling of the melt revealed three types of morphology. At low supercooling of the melt (0.01-0.05) formed the "classic" dendrites, whose form is determined by the anisotropy of the kinetic coefficient (Fig. 2). As the figure shows, the distance between the secondary branches of dendrites decreases with increasing supercooling of the melt.

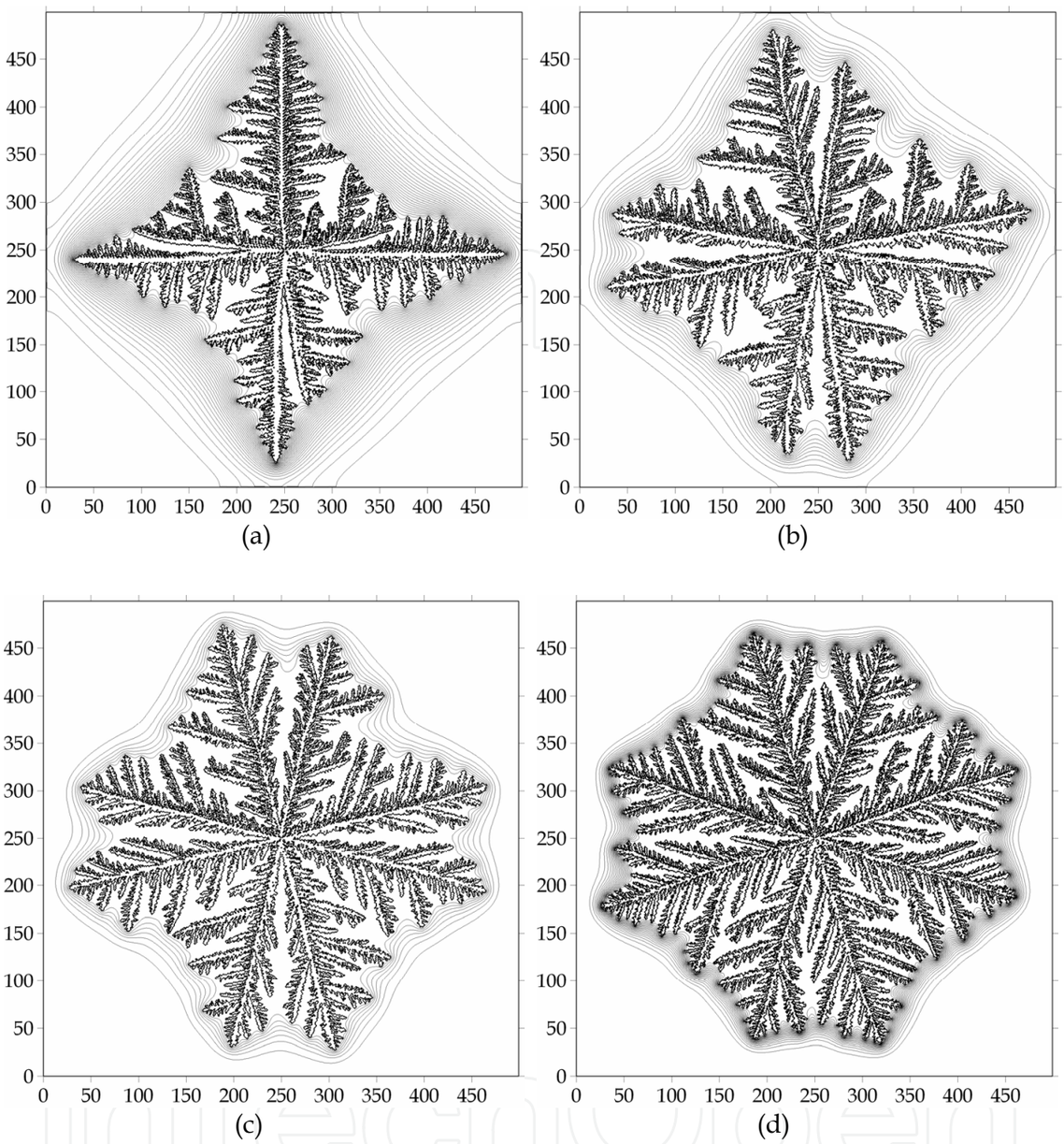

Fig. 4. Morphology of dissipative structures are formed during *Fe-B* melt crystallization and concentration fields (thin lines) in the system in some moments of the time $\tilde{t}$ for various values of bath supercooling $\Delta\tilde{T}_{bath}$: (a) $\Delta\tilde{T}_{bath}$ = 0.055, $\tilde{t}$ = 75; (b) $\Delta\tilde{T}_{bath}$ = 0.065, $\tilde{t}$ = 75; (c) $\Delta\tilde{T}_{bath}$ = 0.080, $\tilde{t}$ = 67; and (d) $\Delta\tilde{T}_{bath}$ = 0.100, $\tilde{t}$ = 62. The isolines of the dimensionless concentration ($\tilde{c}$) were plotted with intervals: (a) $\Delta\tilde{c}$ = 0.02, (b) $\Delta\tilde{c}$ = 0.05, (c) $\Delta\tilde{c}$ = 0.10, and (d) $\Delta\tilde{c}$ = 0.05, respectively.

However, at a further increase in supercooling of the melt a classic form of the dendrite tip becomes unstable. The tip of the dendrite splits {bifurcates). Appears branching the tips of the dendrite (Fig. 3). With further increase of supercooling of the melt (starting with $\Delta\tilde{T}_{bath}$ > 0.050) morphology of dissipative structures acquire a fractal character (formed the "fractal"

dendrites, Fig. 4), which gradually evolving into a globular forms (formed "spherulitic" dendrites, Fig. 5).

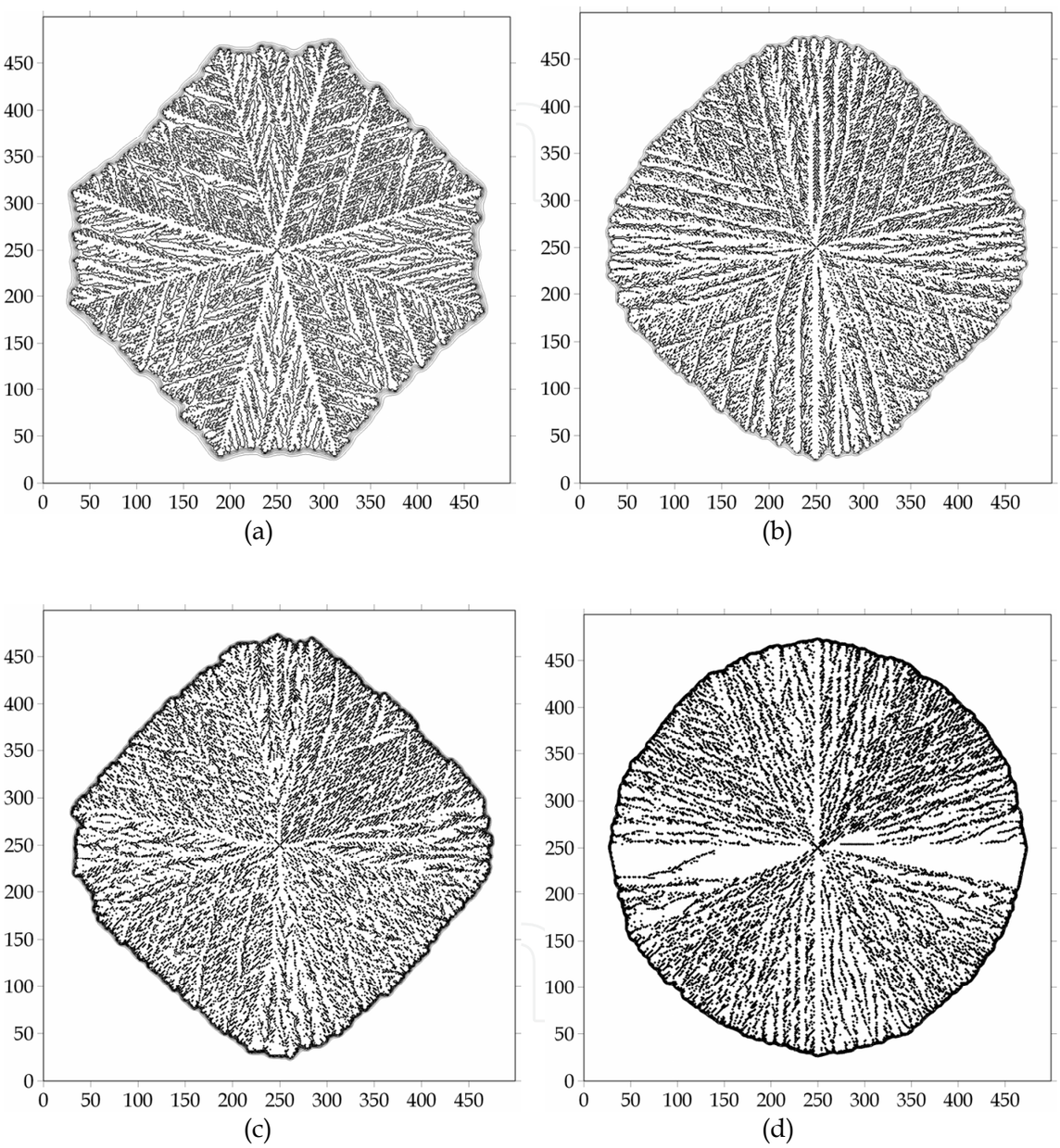

Fig. 5. Morphology of dissipative structures are formed during *Fe-B* melt crystallization and concentration field (thin lines) in the system in some moments of the time $\tilde{t}$ for various values of bath supercooling $\Delta\tilde{T}_{bath}$: (a) $\Delta\tilde{T}_{bath}$ = 0.200, $\tilde{t}$ = 5.80; (b) $\Delta\tilde{T}_{bath}$ = 0.280, $\tilde{t}$ = 4.00; (c) $\Delta\tilde{T}_{bath}$ = 0.430, $\tilde{t}$ = 2.40; and (d) $\Delta\tilde{T}_{bath}$ = 0.535, $\tilde{t}$ = 2.20. The isolines of the dimensionless concentration ($\tilde{c}$) were plotted with intervals: (a) $\Delta\tilde{c}$ = 0.20, (b) $\Delta\tilde{c}$ = 0.20, (c) $\Delta\tilde{c}$ = 0.55, and (d) $\Delta\tilde{c}$ = 0.50, respectively.

The figure 3 shows the initial stage of crystal growth. Are seen differences of the concentration fields of the solute in the melt near the sharp and in the split tops of the dendrite. Growth rate of acute vertices of the dendrite is greater than its bifurcated tops. During further growth of the dendrite is a continuous branching its tops and trunks.

These figures show that with increasing supercooling of the melt increases the degree of branching of dendrites and decreases the length of the diffusion field the concentration of solute component in the melt.

At supercooling of the melt in which the formation of globular growth forms ("spherulitic" dendrite) the region of the diffusion changes in the concentration of the dissolved component is almost completely (entirely) are localized within the macroscopic solidification front (not beyond the radius of the "spherulitic" dendrite).

With the growth process development of the solid phase (with increasing the radius of "spherulitic" dendrite) decreases the curvature of the macroscopic surface of the crystallization front. This leads to the loss of morphological stability of the dissipative structure, to reduced the overall rate of phase transformation in terms of diffusion-limited growth of the solid phase and is responsible for the transition to a kinetic regime of growth under condition when the crystal growth controlled by processes of heat transfer in a system.

Observed in computer modeling of the evolution of the morphology of dissipative structures, formed during the solidification of a supercooled melts, is in full agreement with the paradigm of self-organized criticality, describing the general laws of the development of nonequilibrium, dynamic nonlinear systems. Its essence is that with the development of a nonlinear system, it will inevitably is approaching to the bifurcation point, its stability decreases, and there are conditions under which a small push can cause an avalanche.

The development of dissipative structures is a manifestation of self-organization in nonequilibrium nonlinear systems, providing a maximum rate of increase of entropy during the phase transformation (the principle of maximum rate of entropy increase). At the crystallization of supercooled binary melt the kinetic of phase transformation in the system is controlled by transport processes of the mass and heat (removal of solute and of heat that are released during the phase transformation at the interface), whose transport coefficients are (coefficients of diffusion and thermal conductivity) differ by three orders of magnitude. This causes the appearance of two cycles in the evolution of the morphology of dissipative structures and the kinetics of phase transformation with increasing supercooling of the melt.

3.2 Morphology of dissipative structures formed during the solidification of a supercooled melt under conditions when the crystal growth controlled by processes of heat and mass transfer in a system

We consider the melt solidification from one centre in a system of 250 × 250 cells with the following calculation parameters: time step $\Delta\tilde{t} = (\upsilon_0^2/\alpha)\Delta t$ = 0.025 and spatial step $\Delta\tilde{h} = (\upsilon_0/\alpha)\Delta h$ = 0.50. In special case the simulation is carried out for the time step $\Delta\tilde{t}$ = 0.0125 and grid spacing $\Delta\tilde{h}$ = 0.25 in a 1200 × 1200 system. The computer simulation is realized for various initial and boundary conditions: the system is at the given supercooling $\Delta T = \Delta T_{bath}$ with adiabatic boundary and the temperature on system boundary decreases from some initial value $T_{init} < T_E$ to $T = T_B$ with the given rate of melt cooling R.

In Fig. 6 show the morphology of the growing crystal and the temperature field (in relative magnitudes *TC/Q*) in the system in certain moments of the time for various values of the bath supercooling. With increase of the bath supercooling the morphology of growth of crystal is changed from the globular form of diffusion–limited growth (Fig. 6 a) to the cellular-dendritic form (Fig. 6 b, c) and, then, to the needle-like (Fig. 6 d) and globular (Fig. 6 e) forms of thermally controlled growth. The change of the morphology from the dendrite with a cellular lateral surface to the needle-like dendrite is shown in Fig. 6 (c).

The change in the crystal growth regimes is illustrated by the corresponding changes in the temperature field configuration. The temperature field (Fig. 6 c, d) indicates that the dendritic growth occurs in a thermally controlled regime. The isotherms are distorted under influence of the crystallization heat releasing. In the melt far from the surface of growing crystal the temperature field is concentric isolines. In the diffusion mode the globular growth form is controlled by mass-transfer of solute in the liquid at the interface. With increase of solidification velocity (with increase of supercooling) the solute trapping increases and thus the role of diffusion as limiting factor decreases (Fig. 6 a, b). Whereas the role of the heat transport as limiting factor raises, and it is the most essential at dendrite tip (Fig. 6 c,d), and at the globular form of the growth (Fig. 6 e). The dendrite - globule morphological transition takes place at the deep supercoolings $\Delta\tilde{T} > \Delta\tilde{T}^{**}$ for which the growth velocity $\tilde{V}$ in a minimum of kinetic coefficient ($\tilde{V}^{-}$ in Fig. 1) equals to the diffusion rate $\tilde{V}_D$. Although the kinetic coefficient is small in this case (i.e., exchange atomic fluxes through the interface are small), the deviation from equilibrium is large, and therefore the globule growth occurs with a high velocity and it is controlled by the removal of the released heat of solidification. The high density of isotherms in Fig. 6 e signifies that the rate of latent heat release at the all surface of crystal during solidification is large. If the rate of latent heat release is greater than the heat removal rate then the temperature increases. The temperature increase leads to a solidification velocity increase at the melt supercoolings $\Delta T > \Delta T_{Vmax}$. Thus the globular growth form is established when the heat realize and removal rates are equal.

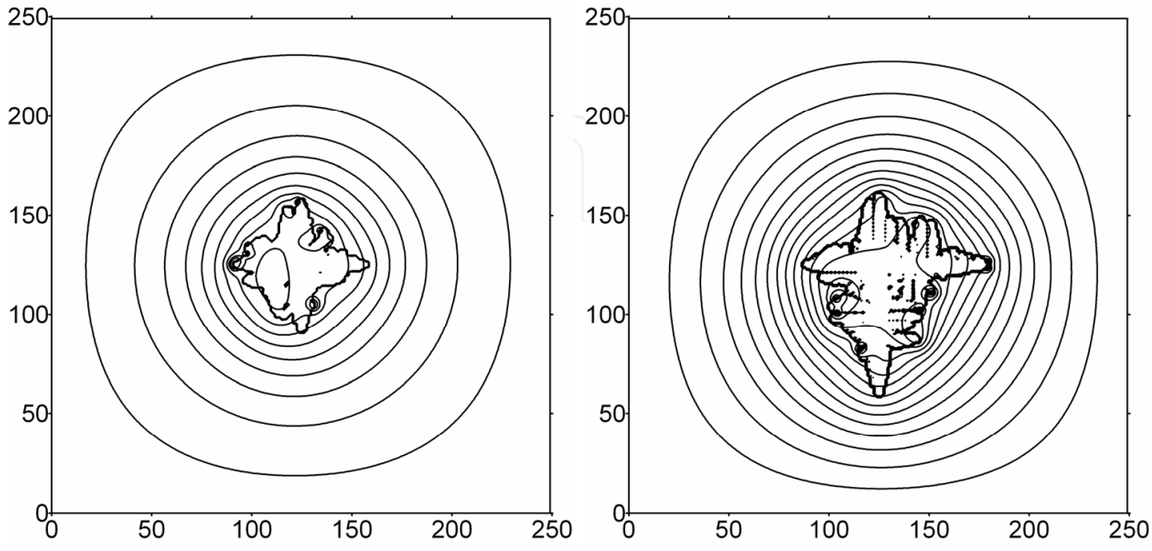

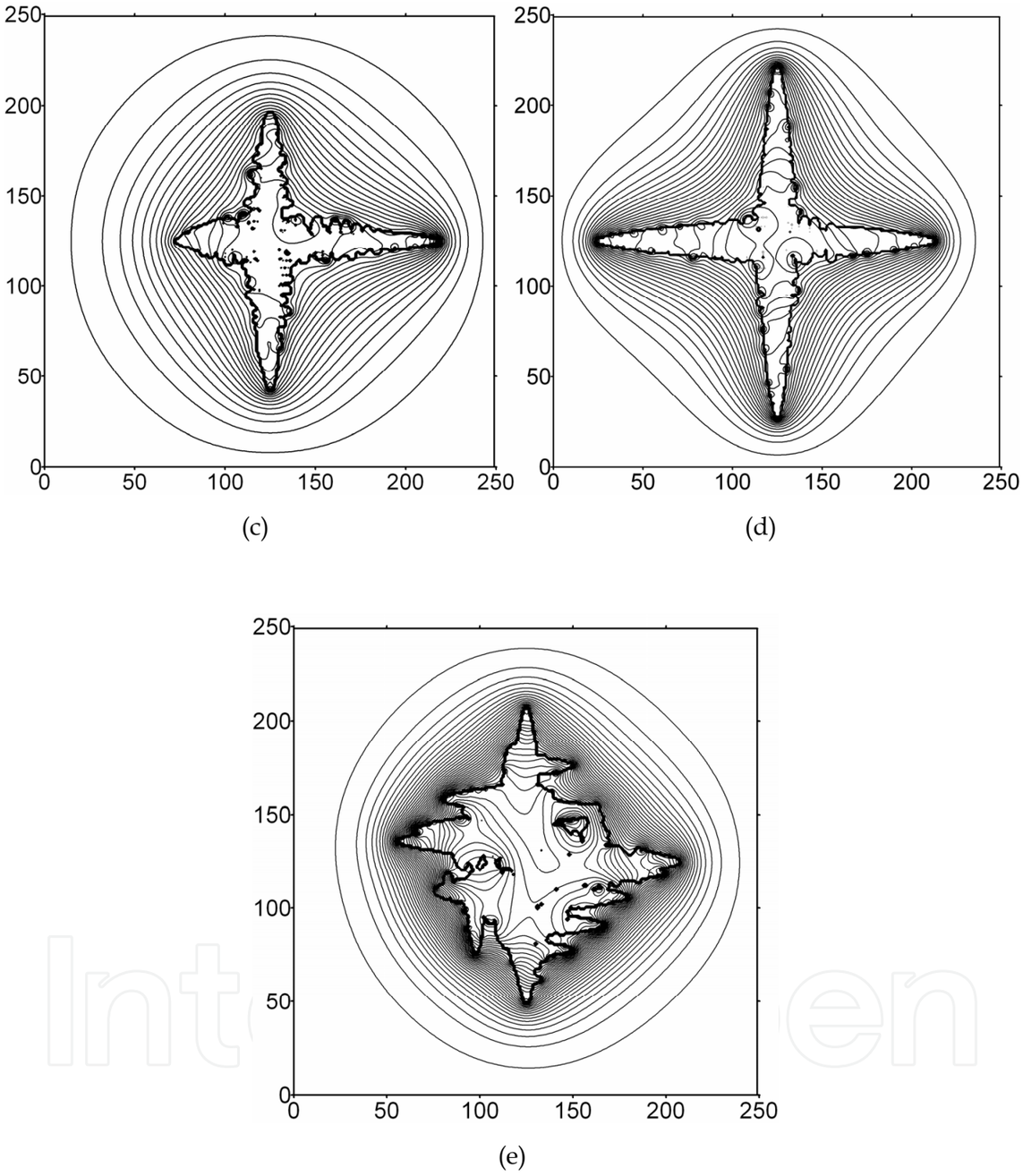

Fig. 6. Morphology of dissipative structures (bold lines) are formed during *Fe-B* melt crystallization and temperature fields (thin lines) in the system in some moments of the time $\tilde{t}$ for various values of bath supercooling $\Delta\tilde{T}_{bath}$: (a) $\Delta\tilde{T}_{bath} = 0.55$, $\tilde{t} = 500$; (b) $\Delta\tilde{T}_{bath} = 0.70$, $\tilde{t} = 500$; (c) $\Delta\tilde{T}_{bath} = 0.75$, $\tilde{t} = 250$; (d) $\Delta\tilde{T}_{bath} = 0.85$, $\tilde{t} = 175$; (e) $\Delta\tilde{T}_{bath} = 1.15$, $\tilde{t} = 250$. The isolines of the dimensionless temperature (TC/Q) were plotted with 0.02 intervals.

Development of instability of interface depends on the local conditions and the influence of temperature and concentration fields of branches in the nonlinear system with feedbacks. In consequence of mutual influence of the temperature and concentration fields of separate branches one of them grow with the deceleration, other is accelerating and thus a selection of the spatial period of the forming structure occurs. The scale of mutual influence of branches essentially changes at the transition from diffusion-controlled to thermally controlled mode of the growth. The sharp increase of the growth velocity of one of branches of the structure formed at the diffusion mode leads to strong distortion of a configuration of a temperature field and as a consequence to chaotic dendritic pattern. It is impossible to exclude completely and the computational grid influence. As the scales of the transfer processes of heat and mass essentially differ, and therefore when the crystallization velocity exceeds the speed of diffusion through border between the neighboring cells ($V \geq D/\Delta h$) the width of a diffusion layer l_D becomes equal to the spatial step of a computational grid ($l_D = \Delta h$).

Morphology of the crystal-melt interface in subsequent moments of the time and the temperature field in the 1200 × 1200 system with the time step $\Delta\tilde{t}$ = 0.0125 and grid spacing $\Delta\tilde{h}$ = 0.25 at $\Delta\tilde{T}_{bath}$ = 0.9 are shown in Fig. 7.

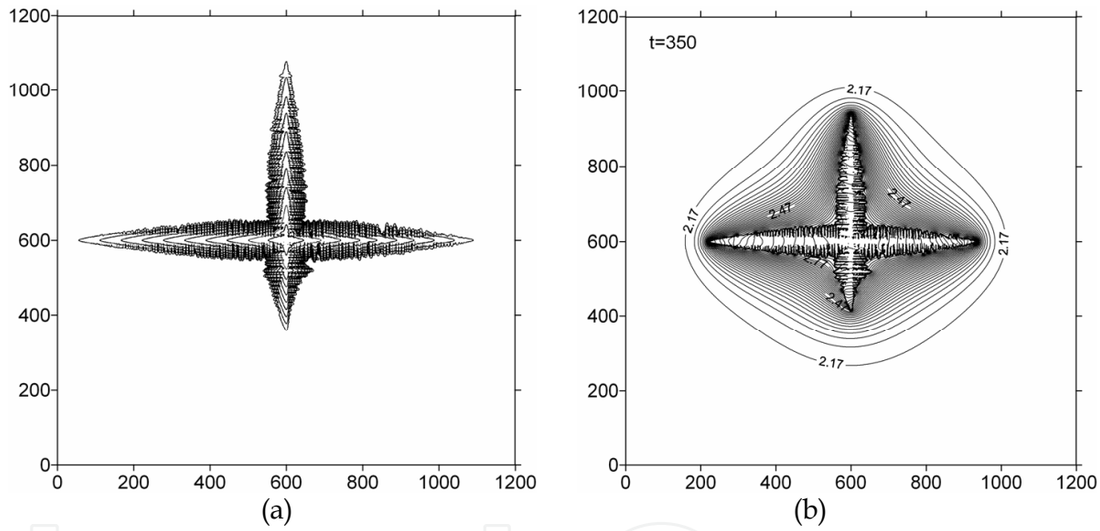

Fig. 7. Morphology of the crystal-melt interface in subsequent moments of the time in a system 1200 × 1200 cells: (a) $\Delta\tilde{T}_{bath}$ = 0.9, $\tilde{t}$ = 50, 100, …, 500. Temperature field in the system: (b) $\Delta\tilde{T}_{bath}$ = 0.9, $\tilde{t}$ =350.

The increase of the system size and the decrease of the grid step give more accurate pattern of side branches far from dendrite tip. At an initial stage of solidification of system all four branches of dendrite grow in a rapid thermal mode. The high rate of latent heat release and the small size of a crystal lead to thermal interaction between branches. As a result of this interaction the growth of one of dendrite branches is decelerated at the moment of time t > 100. The transition to cellular-dendrite growth occurs.

To study the dynamic behavior of interface during the evolution of the *Fe-B* system the change of the crystallization velocity $\tilde{V}$ and supercooling $\Delta\tilde{T}$ at the dendrite tip is calculated. Trajectories of the dendrite tip in the space of variables $\tilde{V}$ and $\Delta\tilde{T}$ are shown in Fig. 8. That is to say this is a phase portrait of a dendrite. Each point corresponds to the state of the interface

($\tilde{V}$, $\Delta\tilde{T}$) in a cell that is on the path of movement of the dendrite tip. The points are obtained by averaging of a supercooling and growth rate over the number of temporary steps, for which the two-phase cell containing the dendrite tip becomes completely solidified. The value of the supercooling ΔT, for which $V = V_D$ in a maximum of kinetic coefficient, is designated as ΔT^* (ΔT^* = 303 K or $\Delta\tilde{T}^*$ = 0.499). Results of computer simulation obtained both under conditions of melt cooling on the system boundaries and under adiabatic boundary conditions show that the V versus ΔT curve has an *S*-like character. The hysteresis characteristic for transition of such type is observed. The bottom branch of solutions is the diffusion mode and the top branch of solutions is the thermal mode. The middle branch of solutions corresponds to cellular or cellular-dendritic growth morphology. This branch corresponds to some intermediate state when the diffusion and thermal modes take place.

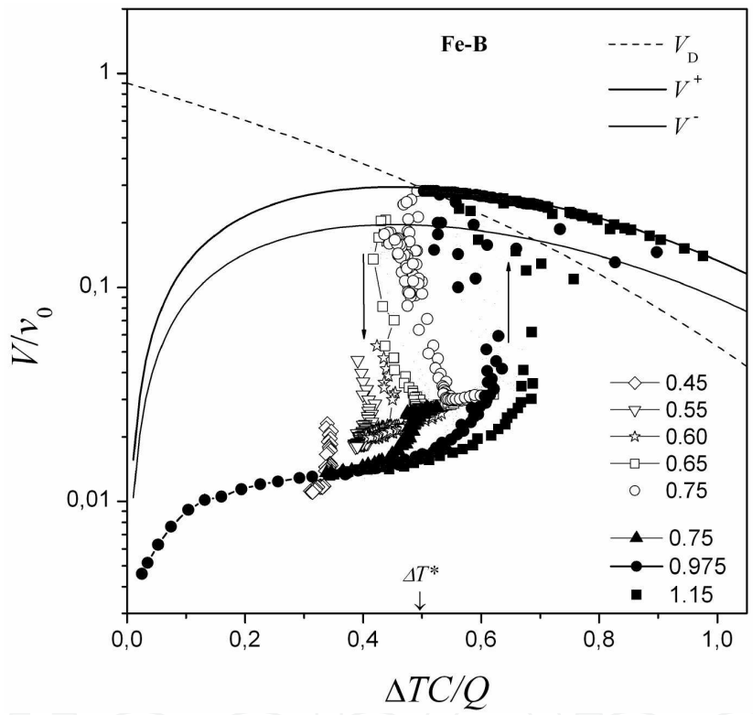

Fig. 8. Dependences of the growth velocity $\tilde{V}$ on supercooling $\Delta\tilde{T}$ of the *Fe-B* melt at dendrite tip. ΔT^* = 303 K. Solid lines: velocity of crystallization in kinetic regime. Solid points: results of simulation obtained under melt cooling on the system boundary with the rate $\tilde{R}$ = 0.001 until $\Delta\tilde{T} = \Delta\tilde{T}_B$. Open points: data of computer simulation of system with initial total supercooling $\Delta\tilde{T} = \Delta\tilde{T}_{bath}$. Values of the total $\Delta\tilde{T}_{bath}$ and final $\Delta\tilde{T}_B$ supercoolings are shown in a legend. Arrows show direction of trajectories of points (in space of variables $\tilde{V}$, $\Delta\tilde{T}$) during dendrite growth.

The growth of crystal at supercooling $\Delta T < \Delta T^*$ is limited by the diffusion of the dissolved component which is rejected by the interface because of a significant separation effect, since the crystallization velocity V is lower than the maximum possible velocity in the kinetic regime $V < V_D$ and, therefore, the partition coefficient k (V) weakly differs from the equilibrium value, which is much smaller than unity. The velocity jump at a dendrite tip

supercooling $\Delta T \geq \Delta T^*$ corresponds to the morphological transition conditioned by the change from a diffusion to a kinetic growth regime controlled by heat transfer in the system. The segregation of dissolved component at the dendrite tip practically is absent, since the partition coefficient $k\,(V)$ is close to unity.

Results of computer simulation with the parameters corresponded approximately to the *Ni-B* system and experimental data on rapid alloy solidification (Eckler at al., 1992) are shown in Fig. 9. To compare our results of computer modeling to experimental data we used values: v_0 = 100 m/s at β_0 = 0.21 m/s K, E_a/RT_E = 5.55, and Q/C = 472.65 K, Θ = 3.651, Q/RT_E = 1.2, k_0 = 0.015 taken from (Eckler at al., 1992). In the experiment the solidification occurs from multitude of the nucleus therefore crystals because of mutual influence morphologically are not developed, but the data on growth velocity specify the onset of the transition to the partitionless regime. The obtained value of a critical supercooling ΔT^* = 244 K on an order of magnitude will be agreed with the experimental data, in particular, for an alloy *Ni* - 1 at % *B* it has been established, that the growth velocity sharply increases and also solidification becomes almost partitionless at critical supercooling ΔT^* = 267 K.

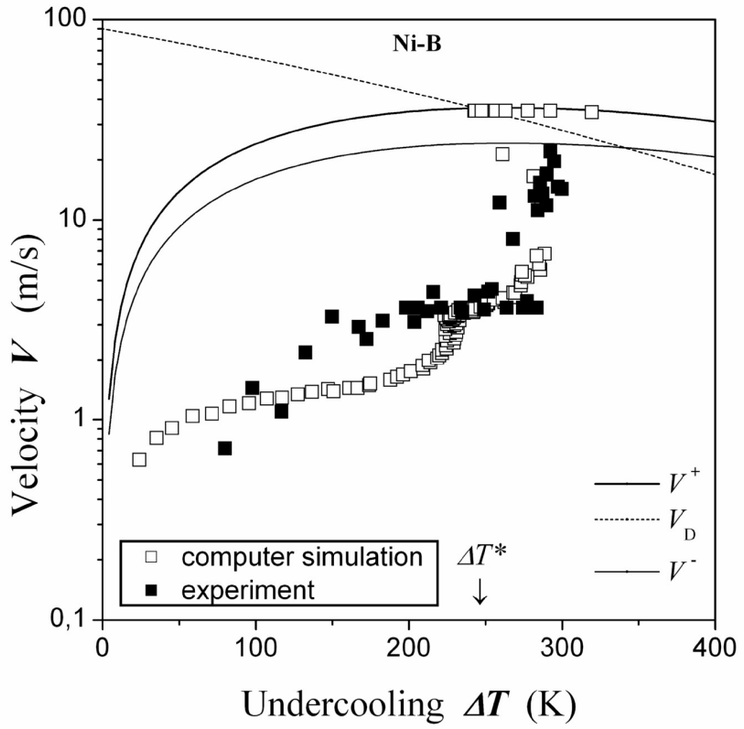

Fig. 9. Dependences of the growth velocity on supercooling of the *Ni-B* melt at dendrite tip. ΔT^* = 244 K. Solid lines: velocity of crystallization in kinetic regime. Open points: results of simulation obtained under melt cooling on the system boundary with the rate $\tilde{R}$ = 0.001 until $\Delta\tilde{T} = \Delta\tilde{T}_B$ =0.9; solid points: data of experiment for *Ni–B*.

4. Conclusion

We have proposed a computer model that takes into account a temperature dependence of diffusion coefficient and a nonequilibrium partition of dissolved component of the alloy. In

this model the dynamics of the formation of dendritic patterns from a crystallization centre has been investigated. The dependence of interface velocity V on an supercooling ΔT at the dendrite tip is obtained during rapid solidification of *Fe-B* and *Ni-B* systems. The morphological transition which is conditioned by change of a diffusion growth mode on thermal growth (dendrites have the form as a needle) at some supercooling at a dendrite tip $\Delta T \geq \Delta T^*$ is detected. The V versus ΔT curve has an S-like character as well as was shown for flat front of crystallization (Galenko & Danilov, 2000) and for parabolic shape of dendrite (Eckler at al., 1994) by analytic methods. Values of a critical supercooling ΔT^* and a growth velocity discontinuity depend on both the anisotropy of the kinetic coefficient, and the difference in the activation energies for atomic kinetics and for diffusion at the interface. The obtained values of a critical supercooling ΔT^* and a growth velocity discontinuity on an order of magnitude agree with well-known experimental data (Eckler at al., 1992).

It is necessary to note, that in the experiment the bath supercooling is measured, and in the present work it is investigated the change of velocity and supercooling at a dendrite tip during the crystallization at the given bath supercooling or the cooling rate. Experimental data for *Ni-B* (Eckler at al., 1992) and recent data for *Ti-Al* (Hartmann at al., 2008) testify that velocity increases with supercooling at a thermal mode. It means, that $\Delta T^* < \Delta T_{Vmax}$. In approach of the given model we obtain for *Ni-B* $\Delta T^* = 244$ K, $\Delta T_{Vmax} = 263$ K and for *Ti-Al* $\Delta T^* = 150$ K, $\Delta T_{Vmax} = 266$ K using material parameters from (Eckler at al., 1992) and (Hartmann at al., 2008), respectively. For more correct comparison with experimental data it is necessary to carry out special modelling taking into account all details of experiment. It was not the purpose of given article.

The proposed computer model allows investigate the solidification of metastable melt at the temperatures in the wide range between the equilibrium liquidus and the glass transition. As it has been noted in (Tarabaev & Esin, 2007), that for enough large rates of cooling the transition to the thermal mode can not be realized, i.e. the system becomes "frozen": when crystal growth is decelerated because recalescence is suppressed and the melt is amorphized (glass transition temperature for the *Fe-B* system is $T_G \sim 0.5\ T_M$ or the supercooling is $\Delta T_G \sim 1.5\ Q/C$ (Elliot, 1983). The crystal growth models with a collision-limited interfacial kinetics are not suitable for the description of alloy solidification at a very large supercooling when a glass formation occurs (Greer, 2001).

5. References

Ahmad, N. A., Wheeler, A. A., Boettinger, W. J., & McFadden, G. B. (1998). Solute trapping and solute drag in a phase-field model of rapid solidification. *Physical Review* E, Vol.58, No.3, pp. 3436-3450, ISSN 1539-3755

Aziz, M. J., & Kaplan, T. (1988). Continuous growth model for interface motion during alloy solidification. *Acta Metallurgica,* Vol.36, pp. 2335-2347, ISSN 0001-6160

Aziz, M. J. (1994). Nonequilibrium Interface Kinetics During Rapid Solidification. *Materials Science and Engineering* A, Vol.178, pp. 167-170, ISSN 0921-5093

Bartel, J., Buhrig, E., Hain, K., & Kuchar, L. (1983). *Kristallisation aus Schmelzen: A Handbook,* K. Hain, E. Buhrig, (Eds.), VEB Deutscher Verlag für Grundstoffindustrie, Leipzig

Chernov, A. A., & Lewis, J. (1967). Computer model of crystallization of binary systems: kinetic phase transitions. *Journal of Physics and Chemistry of Solids,* Vol.28, No.11, pp. 2185-2198, ISSN 0022-3697

Chernov, A. A. (1980). Crystallization processes. In: *Modern Crystallograph,* B.K. Vainshtein, (Ed.), Vol.3, pp. 7-232, Nauka, Moscow, USSR, Russian Federation

Eckler, K., Cochrane, R. F., Herlach, D. M., Feuerbacher, B., & Jurisch, M. (1992). Evidence for a Transition from Diffusion-Controlled to Thermally Controlled Solidification in Metallic Alloys. *Physical Review* B, Vol.45, pp. 5019-5022, ISSN 1098-0121

Eckler, K., Herlach, D. M., & Aziz, M. J. (1994). Search for a Solute-Drag Effect in Dendritic Solidification. *Acta Metallurgica et Materialia,* Vol.42, pp. 975-979, ISSN 0956-7151

Elliot, R. (1983). *Eutectic Solidification Processing: crystalline and glassy alloys.* Butterworths, London, Boston, ISBN 0-408-107146.

Greer, A. L. (2001). From metallic glasses to nanocrystalline solids. *Proc. of 22nd Risø Int. Symp. on Materials Science: Science of Metastable and Nanocrystalline Alloys Structure, Properties and Modelling (Risø National Laboratory Roskilde Denmark 2001),* pp. 461-466

Galenko, P. K., & Danilov, D. A. (2000). Selection of the dynamically stable regime of rapid solidification front motion in an isothermal binary alloy. *Journal of Crystal Growth*, Vol.216, No.1-4, pp. 512–526, ISSN 0022-0248

Hansen, M., & Anderko, K. (1958). *Constitution of Binary Alloys.* McGraw-Hill Book Company, INC, New York, Toronto, London

Hartmann, H., Galenko, P. K., Holland-Moritz, D., Kolbe, M., Herlach, D. M., & Shuleshova, O. (2008). Nonequilibrium solidification in undercooled Ti[sub 45]Al[sub 55] melts. *Journal of Applied Physics*, Vol.103, No.7, pp. 073509-073518, ISSN 0021-8979

Kittl, J. A., Sanders, P. G., Aziz, M. J., Brunco, D. P., & Thompson, M. O. (2000). Complete Experimental Test for Kinetic Models of Rapid Alloy Solidification. *Acta Materialia,* Vol.48, pp. 4797-4811, ISSN 1359-6454

Miroshnichenko, I. S. (1982). *Quenching from the liquid state,* Metallurgiya, Moscow, USSR

Nikonona, V. V., & Temkin, D. E. (1966). Dendrite growth kinetics in some binary melts, In: *Growth and Imperfections of Metallic Crystals,* D.E.Ovsienko, (Ed.), pp. 53-59, Naukova Dumka, Kiev, USSR

Ramirez, J. C., Beckermann, C., Karma, A., & Diepers, H.-J. (2004). Phase-field modeling of binary alloy solidification with coupled heat and solute diffusion. *Physical Review* E, Vol.69, No.5, pp. 051607-051616, ISSN 1539-3755

Tarabaev, L. P., Mashikhin, A. M., & Vdovina, I. A. (1991). Computer simulation of dendritic crystal growth. *VINITI,* Moscow, No. 2915-V91

Tarabaev, L. P., Mashikhin, A. M., & Esin, V. O. (1991). Dendritic crystal growth in supercooled melt. *J. Crystal Growth,* Vol. 114, No. 4, pp. 603 – 612, ISSN 0022-0248

Tarabaev, L. P., Psakh'e, S. G., & Esin, V. O. (2000). Computer Simulation of Segregation, Plastic Deformation, and Defect Formation during Synthesis of Composite Materials. T*he Physics Metals and Metallography*, Vol.89, No.3, pp. 217 – 224, ISSN 0031-918X

Tarabaev, L. P., & Esin, V. O. (2001). Formation of Dendritic Struture upon Directional Solidification of Ternary Alloys. *Russian Metallurgy (Metally),* Vol.2001, No.4, pp. 366- 372, ISSN 0036-0295

Tarabaev, L. P., & Esin, V. O. (2007). Computer Simulation of the Crystal Morphology and Growth Rate during Ultrarapid Cooling of an *Fe-B* Melt. *Russian Metallurgy (Metally),* Vol.2007, No.6, pp. 478-483, ISSN 0036-0295

Temkin, D. E. (1970). Kinetic phase transition at the phase transition in binary alloys. *Kristallografiya*, Vol.15, No.5, pp. 884-893, ISSN 0023-4761

Wheeler, A. A., Boettinger, W. J., & McFadden, G. B. (1993). Phase-field model of solute trapping during solidification. *Physical Review* E, Vol.47, No.3, pp. 1893-1909, ISSN 1539-3755

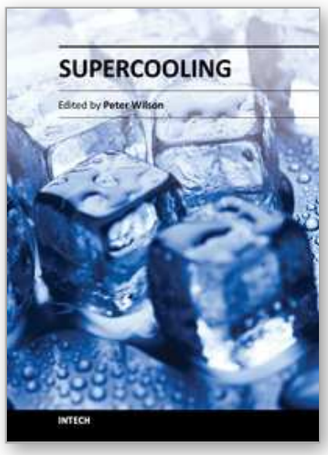

Supercooling

Edited by Prof. Peter Wilson

ISBN 978-953-51-0113-0

Hard cover, 134 pages

Publisher InTech

Published online 09, March, 2012

Published in print edition March, 2012

Supercooled liquids are found in the atmosphere, in cold hardy organisms, in metallurgy, and in many industrial systems today. Stabilizing the metastable, supercooled state, or encouraging the associated process of nucleation have both been the subject of scientific interest for several hundred years. This book is an invaluable starting point for researchers interested in the supercooling of water and aqueous solutions in biology and industry. The book also deals with modeling and the formation subsequent dendritic growth of supercooled solutions, as well as glass transitions and interface stability.

How to reference

In order to correctly reference this scholarly work, feel free to copy and paste the following:

Leonid Tarabaev and Vladimir Esin (2012). Formation of Dissipative Structures During Crystallization of Supercooled Melts, Supercooling, Prof. Peter Wilson (Ed.), ISBN: 978-953-51-0113-0, InTech, Available from: http://www.intechopen.com/books/supercooling/formation-of-dissipative-structures-during-crystallization-of-supercooled-melts-

INTECH
open science | open minds

InTech Europe
University Campus STeP Ri
Slavka Krautzeka 83/A
51000 Rijeka, Croatia
Phone: +385 (51) 770 447
Fax: +385 (51) 686 166
www.intechopen.com

InTech China
Unit 405, Office Block, Hotel Equatorial Shanghai
No.65, Yan An Road (West), Shanghai, 200040, China
中国上海市延安西路65号上海国际贵都大饭店办公楼405单元
Phone: +86-21-62489820
Fax: +86-21-62489821

IntechOpen